



**HAL**  
open science

## From Stilbenes to carbo-Stilbenes: an Encouraging Prospect

Chongwei Zhu, Alix Sournia-Saquet, Valérie Maraval, Christian Bijani,  
Xiuling X Cui, Albert Poater, Remi R Chauvin

► **To cite this version:**

Chongwei Zhu, Alix Sournia-Saquet, Valérie Maraval, Christian Bijani, Xiuling X Cui, et al.. From Stilbenes to carbo-Stilbenes: an Encouraging Prospect. *Chemistry - A European Journal*, 2024, 30 (26), pp.e202400451. 10.1002/chem.202400451 . hal-04532883

**HAL Id: hal-04532883**

**<https://hal.science/hal-04532883v1>**

Submitted on 4 Apr 2024

**HAL** is a multi-disciplinary open access archive for the deposit and dissemination of scientific research documents, whether they are published or not. The documents may come from teaching and research institutions in France or abroad, or from public or private research centers.

L'archive ouverte pluridisciplinaire **HAL**, est destinée au dépôt et à la diffusion de documents scientifiques de niveau recherche, publiés ou non, émanant des établissements d'enseignement et de recherche français ou étrangers, des laboratoires publics ou privés.



Distributed under a Creative Commons Attribution 4.0 International License

# From Stilbenes to *carbo*-Stilbenes: an Encouraging Prospect

Chongwei Zhu,<sup>[a, b]</sup> Alix Saquet,<sup>[c]</sup> Valérie Maraval,<sup>[c]</sup> Christian Bijani,<sup>[c]</sup> Xiuling Cui,<sup>[d]</sup> Albert Poater,<sup>\*[e]</sup> and Remi Chauvin<sup>\*[a, d]</sup>

Dedicated to Prof. Miquel Solà for his 60th Anniversary

Beyond previously described *carbo*-naphthalene and *carbo*-biphenyl, a novel type of bis-*carbo*-benzenic molecules is envisaged from the stilbene parent. The synthesis, structure, spectroscopic and electrochemical properties of two such *carbo*-stilbenes are described at complementary experimental and computational DFT levels. In the selected targets, the bare skeletal *carbo*-mer of *carbo*-stilbene is decorated by 8 or 10 phenyl groups, 0 or 2 *tert*-butyl groups, and 2 *n*-octyl chains, the later substituents being introduced to compensate anticipated solubility issues. As in the parent stilbene series, isomers of the phenylated *carbo*-stilbenes are characterized. The *cis*- and *trans*-isomers are, however, formed in almost equal amounts and could not be separated by either chromatography or crystallization. Nevertheless, due to a slow interconversion at the NMR time scale (up to 55 °C) the <sup>1</sup>H NMR signals of both isomers of the two *carbo*-stilbenes could be tentatively

assigned. The calculated structure of the *cis*-isomer exhibits a helical shape, consistent with the observed magnetic shielding of phenyl *p*-CH nuclei residing inside the shielding cone of the facing C<sub>18</sub> ring. The presence of the two isomers in solution also gives rise to quite broad UV-vis absorption spectra with main bands at *ca* 460, 560 and 710 nm, and a significant bathochromic shift for the decaphenylated *carbo*-stilbene *vs* the di-*tert*-butyl-octaphenylated counterpart. Square wave voltammograms do not show any resolution of the two isomers, giving a reversible reduction wave at −0.65 or −0.58 V/SCE, and an irreversible oxidation peak at 1.11 V/SCE, those values being classical for most *carbo*-benzene derivatives. Calculated NICS values (NICS(1) = −12.5 ± 0.2 ppm) also indicate that the aromatic nature of the C<sub>18</sub> rings is not markedly affected by the dialkynylbutatriene (DAB) connector between them.

## Introduction

The C<sub>14</sub> skeleton of stilbene (C<sub>6</sub>H<sub>5</sub>—CH=CH—C<sub>6</sub>H<sub>5</sub>) occurs in numerous natural and synthetic products with various prospects of applications in life, chemical, and materials science,<sup>[1]</sup> thanks to their therapeutic,<sup>[2]</sup> chromophoric, and photo-isomerization properties,<sup>[3]</sup> respectively.

Within the context of the recent focus of *carbo*-mer<sup>[4a]</sup> chemistry<sup>[4b–g]</sup> on derivatives containing two annulated or catenated C<sub>18</sub> *carbo*-benzenic rings at least (*carbo*-naphthalene skeleton **A**,<sup>[5]</sup> *carbo*-biphenyl skeleton **B**<sup>[6]</sup>), the C<sub>44</sub> skeletal *carbo*-mer of stilbene **C** (C<sub>18</sub>H<sub>5</sub>—C≡C—CH=C=C—CH—C≡C—C<sub>18</sub>H<sub>5</sub>) emerges as an imperious target to be studied by both experimental and computational methods (Figure 1a). Contrary to tolane (C<sub>6</sub>H<sub>5</sub>—C≡C—C<sub>6</sub>H<sub>5</sub>) and *carbo*-biphenyl **B** (C<sub>18</sub>H<sub>5</sub>—C≡C—C<sub>18</sub>H<sub>5</sub>), the so-called fictitious *carbo*-stilbene **C** is likely to exhibit the same stereoisomerism as stilbene in the Eliel's sense,<sup>[7]</sup> under either *cis*- (*Z*) or *trans*- (*E*) configuration through the [3]cumulene linker. From a general standpoint, acyclic [*n*]cumulenes R<sup>1</sup>R<sup>2</sup>C=(C)<sub>*n*−1</sub>=CR<sup>1</sup>R<sup>2</sup> were long studied for their bond-length alternation (BLA), and their cumulenic rotation barrier (CRB) corresponding to *R/S* enantiomerization for even *n* and *cis(Z)/trans(E)* diastereo-conversion for odd *n*.<sup>[8,9]</sup> Given a substituent set, both BLA and CRB are anticipated to decrease *vs n* and parity of *n* due to the relative stabilization of the open shell diradical form R<sup>1</sup>R<sup>2</sup>C•—(C)<sub>*n*−1</sub>—C•R<sup>1</sup>R<sup>2</sup>.<sup>[10]</sup> In the odd series, the [3]cumulene (or butatriene) motif has attracted special attention due to its second position after the alkene

[a] Dr. C. Zhu, Prof. R. Chauvin

Faculté Science et Ingénierie - Département de Chimie. Unsaturated molecules for physics, biology and chemistry group. Université Toulouse III - Paul Sabatier, 118 route de Narbonne, 31-062 Toulouse Cedex 09, France  
E-mail: remi.chauvin@univ-tlse3.fr

[b] Dr. C. Zhu

Key Laboratory of Functional Molecular Solids, Ministry of Education, and School of Chemistry and Materials Science, Anhui Normal University, Wuhu 241002, China

[c] Dr. A. Saquet, Dr. V. Maraval, Dr. C. Bijani

LCC-CNRS, Université de Toulouse, CNRS, UPS, Toulouse, France

[d] Prof. X. Cui, Prof. R. Chauvin

Engineering Research Center of Molecular Medicine of Ministry of Education, Key Laboratory of Fujian Molecular Medicine, Key Laboratory of Xiamen Marine and Gene Drugs, School of Biomedical Sciences, Huaqiao University, Xiamen 361021, China

[e] Dr. A. Poater

Institut de Química Computacional i Catàlisi, Departament de Química, Universitat de Girona, c/ M<sup>a</sup> Aurèlia Capmany 69, 17003 Girona, Catalonia, Spain  
E-mail: albert.poater@udg.edu  
Homepage: <http://iqcc.udg.edu/wordpress/portfolio/albert-poater/>

Supporting information for this article is available on the WWW under <https://doi.org/10.1002/chem.202400451>

© 2024 The Authors. Chemistry - A European Journal published by Wiley-VCH GmbH. This is an open access article under the terms of the Creative Commons Attribution License, which permits use, distribution and reproduction in any medium, provided the original work is properly cited.

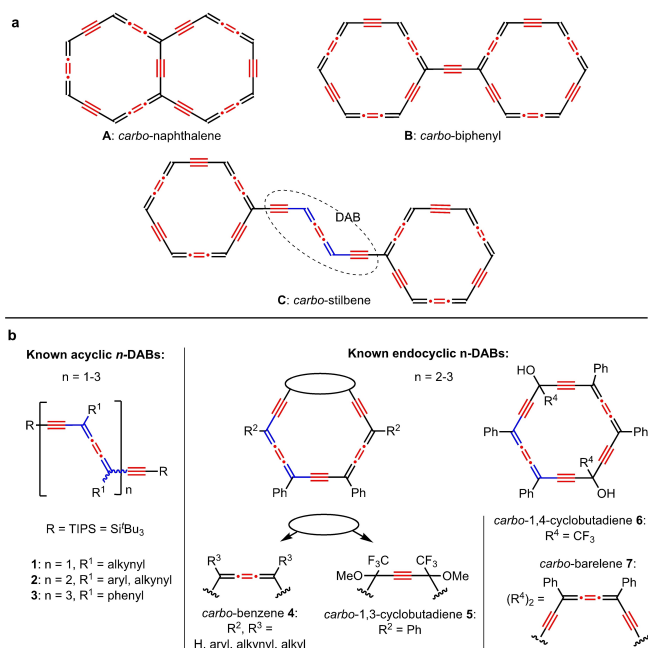


**Figure 1.** a) Exemplified bis-carbo-benzenic structures **A**, **B**, and carbo-stilbene target **C**; b) known acyclic and cyclic oligo-dialkynylbutatrienes (*n*-DABs,  $n = 1-3$ ).

motif, and its specific nature as the *carbo*-mer of the latter.<sup>[7,11]</sup> In the *carbo*-stilbene structure **C**, the two *carbo*-benzene rings are conjugated through a particular [3]cumulene connector, i.e. a dialkynyl-butatriene (DAB) unit. In contrast to the ethynylene  $C_2$  connector of stilbene, the  $C_8$  DAB unit is known to undergo facile *cis*  $\rightleftharpoons$  *trans* isomerization, with small thermodynamic preference for either isomer due to the absence of steric interaction between remote substituents.<sup>[12,13,14]</sup>

Regardless of stereochemistry, the kinetic stability of acyclic DABs **1** was shown to increase with the substituent bulkiness (Figure 1b).<sup>[14,15,16,17]</sup> In fused acyclic oligo-DABs (*n*-DABs), *carbo*-butatrienes **2** ( $n = 2$ ) were also shown to be quite stable when protected by bulky silyl groups,<sup>[2c]</sup> while the *carbo*-hexatriene **3** ( $n = 3$ ) could be isolated and stored in the solid state only, as an unfrozen *cis-trans* stereochemical mixture.<sup>[18,19]</sup> The *cis*  $\rightarrow$  *trans* isomerization is however frozen in endocyclic *n*-DABs, such as aromatic *carbo*-benzenes **4** ( $n = 3$ ) where the alternating butatriene and butyne edges of the equivalent Kekule structures provide the three DAB units with a “hemi-butatriene” character.<sup>[9]</sup> In non-aromatic cyclic *n*-DABs, the two butatriene units of *carbo*-1,3-cyclohexadienes **5** are  $\pi$ -conjugated through the fusing triple bond (as in acyclic *carbo*-butatrienes **2**),<sup>[20]</sup> while the two  $\pi$ -independent DAB motifs of *carbo*-1,4-cyclohexadienes **6** ( $n = 2$ )<sup>[21]</sup> or *carbo*-barrelene **7** ( $n = 3$ )<sup>[22]</sup> are homo-conjugated through two  $sp^3$ -C atoms (Figure 1).

As the *n*-DABs **1–7** were shown to be chemically quite stable, and  $sp^2$ C-unsubstituted DABs ( $R-C\equiv C-CH=C=C=CH-C\equiv C-R$ ) and *carbo*-benzene ( $C_{18}H_6$ ) remain unknown,<sup>[4,23]</sup> per-substituted derivatives of **C** appeared as reasonable objectives. Considering the large size and synthesis efficiency of

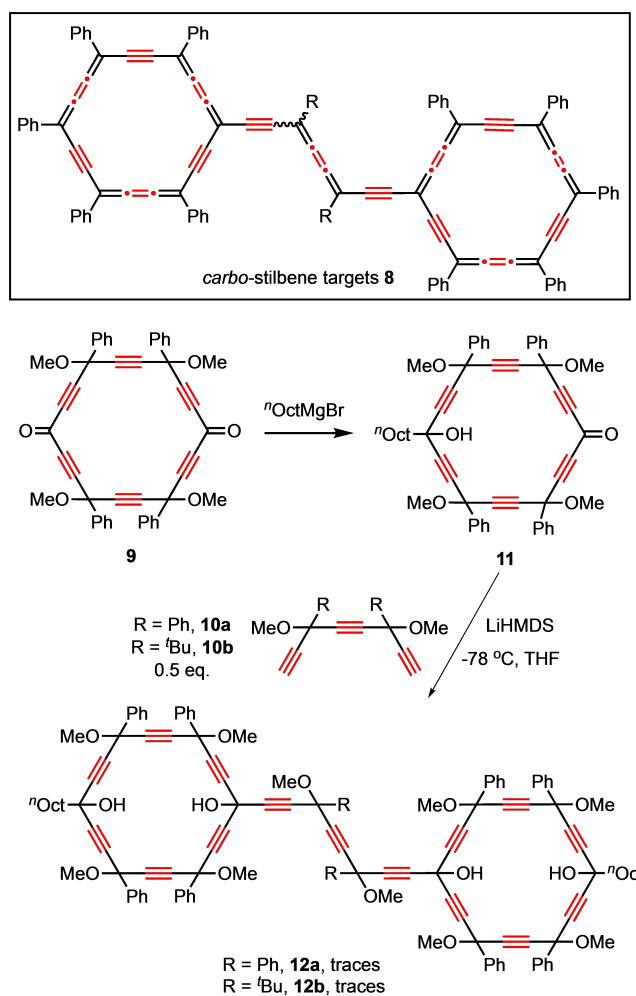
tetraphenyl-*carbo*-benzenes,<sup>[4e–9]</sup> the *carbo*-stilbenes **8a–b** were devised as optimal first targets (Scheme 1).

## Results and Discussion

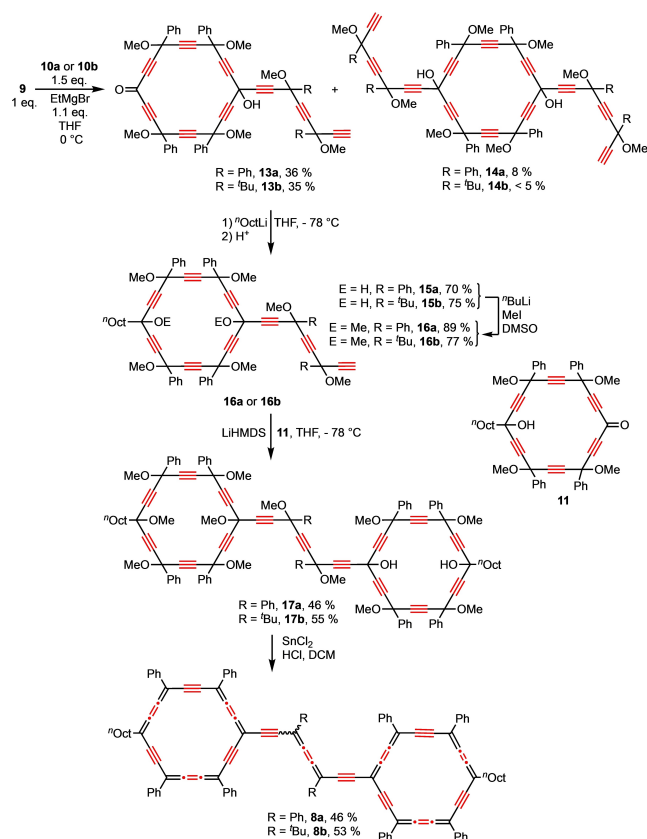
The preparation of *carbo*-stilbenes **8** was envisaged from the [6]pericyclonydione **9**<sup>[24]</sup> by successive nucleophilic additions, as previously experienced for the synthesis of *n*-octyl-substituted *carbo*-biphenyl (**B**, Figure 1) and *carbo*-terphenyl derivatives.<sup>[6]</sup> All the starting materials or products described below were used or obtained as statistical mixtures of stereoisomers.

In a first attempt (Scheme 1), addition of the triyne **10a**<sup>[24]</sup> or **10b**<sup>[25]</sup> to two equivalents of the known [6]pericyclonydione **11**, obtained by addition of one equivalent of *n*-octylmagnesium bromide to the diketone **9**,<sup>[6]</sup> gave only trace amounts of the double adduct **12a** or **12b**. An alternative strategy was thus considered (Scheme 2).

Addition of the mono-bromomagnesium salts of the triyne **10a–b** (generated from 1.5 equivalent of triyne and 1.1 equivalent of EtMgBr) to a single equivalent of diketone **9** was found to be an efficient method to obtain the monoadduct



**Scheme 1.** *Carbo*-stilbene targets **8**, and first attempt at synthesis thereof.

Scheme 2. Synthesis of the *carbo*-stilbenes **8a** and **8b**.

**13a–b** as major product, accompanied with minor quantities of the diadduct **14a–b**, along with unreacted diketone **9** and triyne **10a–b** (Scheme 2). The monoketone **13a–b** was then treated with *n*-octyllithium to give the diol **15a–b**, which was subsequently di-*O*-methylated to the octaether **16a–b**. Finally, addition of **16a–b** to the monoketone **11** in the presence of LiHMDS afforded the key bis-hexaoxy[6]pericylyne **17a–b** with 46–55% yields. Ultimate acidic reductive treatment of **17a–b** with SnCl<sub>2</sub>/HCl allowed isolation of the *carbo*-stilbene **8a–b** with 46–53% yield, i.e. with 89–91% average yield for each of the seven butatriene edges formed in **8a–b**. The two *carbo*-stilbenes were isolated as black solids and found to be stable in solution, albeit poorly soluble despite the presence of two *n*-octyl chains, and two extra *tert*-butyl groups in **8b**, both types of substituents being previously reported to increase the solubility of *carbo*-benzene derivatives.<sup>[6,25]</sup>

The low solubility of both the *carbo*-stilbenes **8a** and **8b** prevented their full characterization, in particular by <sup>13</sup>C NMR spectroscopy. <sup>1</sup>H and <sup>1</sup>H-<sup>1</sup>H COSY NMR spectra could however be recorded, and <sup>1</sup>H-<sup>13</sup>C HSQC and HMBC experiments (at 600 MHz, 45 °C) could also be recorded for the slightly more soluble *carbo*-stilbene **8b**. The results allowed a tentative assignment of all the <sup>1</sup>H NMR signals, in spite of their duplication due to the simultaneous presence of the *cis*- and *trans*- isomers, the diastereomeric ratio being *ca* 52:48 for **8a**, 56:44 for **8b** (Figure 2 and S.I.).

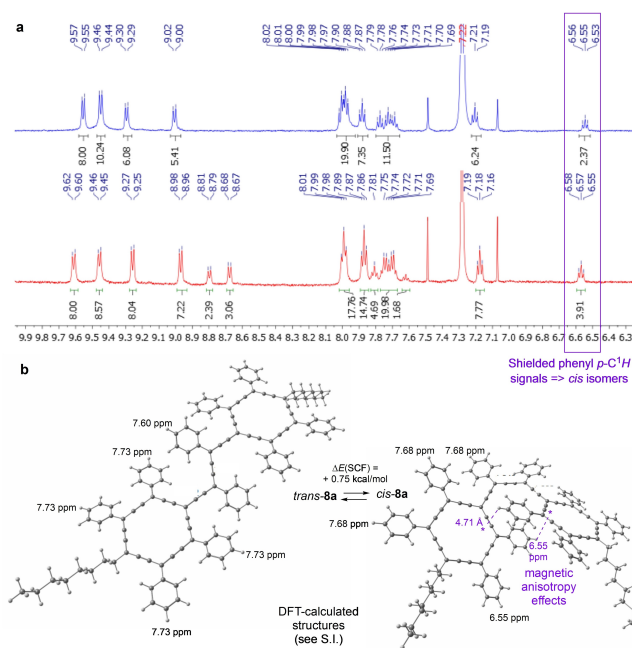


**Figure 2.** a) Aromatic region of <sup>1</sup>H NMR spectra of the *carbo*-stilbenes **8a** (R = Ph, *bottom*) and **8b** (R = <sup>t</sup>Bu, *top*), in CDCl<sub>3</sub> solution (500 MHz, 55 °C). b) DFT-calculated equilibrium structures of *cis*-**8a** and *trans*-**8a** (see Table S4), possibly accounting for magnetic shielding effects on the *p*-C<sup>1</sup>H nuclei of phenyl substituents made chemically inequivalent by restricted rotation of the C<sub>18</sub> rings with respect to the central DAB connector.

From systematic variable temperature NMR experiments at 500 MHz, noteworthy is the absence of signal coalescence between 25 and 55 °C, suggesting that the stereo-conversion barrier should be greater than 20 kcal/mol. Owing to the extremely poor solubility of **8a** and **8b** in solvents other than CD<sub>2</sub>Cl<sub>2</sub> or CDCl<sub>3</sub> and known thermal sensitivity of non-end aromatic butatriene derivatives, recording spectra at higher temperatures would not be feasible.

The most striking observation for one of the isomers (and only one, assigned to *cis*-**8a** or *cis*-**8b**) is the degeneracy lift of pairs of phenyl substituents, suggesting a blockage of the free rotation about the DAB–C<sub>18</sub> single bonds, which is allowed in the *trans*-isomer only. This is actually markedly evidenced in Density Functional Theory (DFT)-calculated isomers of **8a** and **8b** (see discussion below, Figure 2b, and legend of Figure 2).

As usually observed for centrosymmetric tetraphenyl-*carbo*-benzenes, the *p*-C<sup>1</sup>H (and *m*-C<sup>1</sup>H) nuclei of adjacent phenyl substituents have identical chemical shifts. Such an equivalence was however unexpected for the internal phenyl groups of *cis*-**8a** (and *cis*-**8b**), whose *p*-C<sup>1</sup>H nuclei both resonate at 6.55 ppm in spite of their different positions from the facing C<sub>18</sub> ring in the calculated structure. This structure being rigid, the observed average equivalence at 55 °C could be tentatively attributed to flexibility in solution incidentally subjecting the two phenyl rings to identical average magnetic anisotropy effects. Moreover, using a classical software, such as NMR predict from Mestrenova 14.1.2-25024, the simulated NMR spectra of **8a** and **8b** are differentially shifted to high field (see S.I.), due to the

fact that specific magnetic anisotropy effect of *carbo*-aromatic rings are not (yet) implemented.

In both  $^1\text{H}$  NMR spectra, deshielded doublet signals above 9 ppm are characteristic of *o*- $\text{C}^1\text{H}$  nuclei of phenyl substituents of *carbo*-benzenes (Figure 2a). At the opposite, a shielded triplet signal at 6.55 ppm is here attributed to *p*- $\text{C}^1\text{H}$  nuclei of particular phenyl groups of the *cis*-isomer: for steric reason, one of phenyl substituents of each  $\text{C}_{18}$  ring in *ortho* position to the DAB linker is indeed expected to lie in the shielding cone of the facing  $\text{C}_{18}$  ring, and *vice-versa*, in agreement with the DFT-calculated equilibrium structures of **8a** and **8b** (see legend of Figure 2 and S.I.). This feature being observed for both **8a** and **8b**, the shielded signals at 6.55 ppm cannot be assigned to the phenyl substituents of the DAB connector of **8a**.

DFT calculations of **8a** and **8b** were thus performed at the B3PW91-D3/6-311G(d,p)-pcm//B3PW91/6-31G(d,p) level, by enforcing  $\text{C}_i$  symmetry and  $\text{C}_2$  symmetry for the *trans* and *cis* stereoisomers, respectively. The calculated Gibbs energy at 298.15 K of the *cis*  $\rightleftharpoons$  *trans* equilibrium opted by  $-0.8$  and  $0.9$  kcal/mol for **8a** and **8b**, respectively. The *cis*  $\rightleftharpoons$  *trans* transition state failed to be located, but energy profiles vs incremental rotation did suggest an energy barrier of at least 20.0 and 18.9 kcal/mol for **8a** and **8b**, respectively (see Table S4).

The *trans*-isomers exhibit classical structural features for both the tetraphenyl-octyl-*carbo*-benzene moieties and their DAB connector. The equilibrium structure of **8a** thus exhibits a roughly planar diphenyl-DAB core (with central and lateral *spC*–*spC* bond distances of 1.248 and 1.222 Å, respectively, and torsion angles of the phenyl substituents of *ca* 5.6°), along with *quasi*-planar  $\text{C}_{18}$  rings (with deviation from the mean plane in the range 0.001–0.043 Å) of slightly dissymmetric hexagonal shape (with *n*-OctC $\cdots$ C(DAB) and PhC $\cdots$ CPh diagonal through-space distances of 8.07 and 7.82 Å, respectively).

As expected from the intramolecular steric hindrance, the *cis*-isomers exhibit a helical structure, with a distorted DAB core (with a global torsion of 9.4°) along with slightly more planar  $\text{C}_{18}$  rings (with deviation from the mean plane in the range 0.001–0.039 Å) of slightly dissymmetric hexagonal shape (with *n*-OctC $\cdots$ C(DAB) and PhC $\cdots$ CPh diagonal distances of 7.796 Å and  $8.087 \pm 0.009$  Å, respectively). Although the internal phenyl substituents at *ortho* positions of the two  $\text{C}_{18}$  rings roughly overlap by parallel mean planes (see Figure 2b), no  $\pi$  stacking could be evidenced, the shortest through-space distances to the facing  $\text{C}_{18}$  ring and to the symmetric phenyl substituent being  $\text{C1}\cdots\text{C2} = 4.567$  Å (where C1 denotes a phenyl *m*-C atom, C2 denotes a *spC* atom of the  $\text{C}_{18}$  ring) and  $\text{C1}'\cdots\text{C2}' = 4.773$  Å (where C1' and C2' denote *o*-C atoms of each phenyl ring), respectively.

Calculations were also made after truncating the octyl chains to methyl groups in simplified versions **8aS1** and **8bS1** (see Table S4), to check possible steric effects on the relative thermodynamic stability or spectroscopic properties. No significant differences were however obtained.

With the view to appraising specific effects of the *carbo*-meric rings and DAB bridge, all the octyl and phenyl substituents were replaced by H atoms in simplified versions

**8S2**, giving rise to almost isoenergetic *cis*- and *trans*-isomers, but still with 0.1 kcal/mol in favor of the *trans* isomer (see Table S4). Nevertheless, the isomerization would still require a minimum of 16.9 kcal/mol.

In an ultimate simplification, the  $\text{C}_{18}$  rings and phenyl DAB substituents of **8a** were replaced by hydrogen atoms in a bare DAB **8S3**, leading to an isomeric preference of 3.3 kcal/mol, while the barrier corresponding to the characterized transition state is reduced to 5.0 kcal/mol.

In conclusion, the isomerization is not impeded by the central butatriene motif itself, but by the *carbo*-benzene rings and substituents thereof.

Knowing the stronger magnetic aromatic character of  $\text{C}_{18}$  rings with respect to  $\text{C}_6$  phenyl rings from previous studies (as indicated by comparison of  $^1\text{H}$  NMR spectra at low field),<sup>[6,22,25]</sup> the local aromaticity of *carbo*-stilbenes was assessed using the nucleus-independent chemical shift (NICS), a metric introduced by Schleyer and colleagues, serving as a general scalar descriptor of algebraic magnetic (anti)aromaticity.<sup>[26]</sup> NICS is defined as the negative absolute shielding value computed at a ring center (NICS(0)), or 1 Å above or below it (NICS(1) and NICS(–1)). Rings exhibiting substantial negative NICS values are identified as aromatic.<sup>[27]</sup> NICS values were determined utilizing the gauge-independent atomic orbital method (GIAO). The magnetic shielding tensor was computed for ghost atoms positioned at the center of the rings (or 1 Å above or below it), as determined by the non-weighted mean of the heavy atom coordinates.<sup>[28]</sup> Calculated NICS values of *carbo*-stilbenes suggest a minimal impact of the DAB connector on the aromatic nature of the  $\text{C}_{18}$  rings. For **8a**, the NICS(1) values at the  $\text{C}_{18}$  rings supports a slightly higher aromaticity in the *trans* isomer than in the *cis*-isomer ( $-12.5$  and  $-12.4$  ppm respectively, to be compared with a similar or identical value of  $-12.5$  ppm for the *carbo*-diphenyl **18**, all being significantly less aromatic than unsubstituted *carbo*-benzene  $\text{C}_{18}\text{H}_6$  ( $-16.8$  ppm). Qualitatively, the trend is the same with the classical NICS(0) index, again not differentiating between the *cis*- and *trans*-isomers for **8a**. The values for *cis*- and *trans*-**8b** are rather similar, but slightly larger in absolute value ( $-12.7$  and  $-12.6$  ppm for the *cis* and *trans* isomers, respectively), correlating with the known  $\pi$ -insulating effect of *tert*-butyl groups with respect to phenyl groups when conjugated to a  $\text{C}_{18}$  ring,<sup>[25]</sup> even through a [3]cumulene linker in the present case. In addition, comparison of the NICS(1) values (Table S3) show that the DAB phenyl substituents of *cis*- and *trans*-**8a** ( $\approx -9.8$  ppm) are more aromatic by *ca* 1 ppm than those of the  $\text{C}_{18}$  rings. Changing two Ph groups by two *tert*-Bu groups from **8a** to **8b**, the average NICS(1) values of the peripheral phenyl and  $\text{C}_{18}$  rings decrease by *ca* 0.2 ppm.

UV-vis absorption spectra of **8a** and **8b** were recorded in chloroform solutions. The two *carbo*-stilbenes exhibit comparable UV-vis spectra with two quite broad intense absorption bands at  $459 \pm 4$  and  $550 \pm 3$  nm, followed by a weaker band at longer wavelength (Figure 3). These spectral profiles are similar to that of the *carbo*-biphenyl **18**,<sup>[6]</sup> in which the two  $\text{C}_{18}$  rings are conjugated by a  $\text{C}_2$  ethynyl linker instead of the  $\text{C}_8$  DAB linker: as expected, the more  $\pi$ -extended DAB linker induces a bathochromic shift. The stronger effect is observed for the small

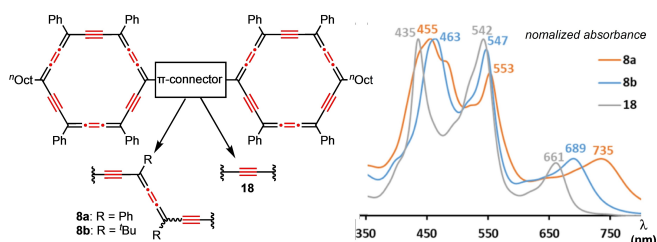


**Figure 3.** Normalized UV-visible absorption spectra of the *carbo*-stilbenes **8a** and **8b** and *carbo*-biphenyl **18** (in degassed  $\text{CHCl}_3$ ).

absorption bands in the 630–740 nm region, with a red shift of 74 nm from the *carbo*-biphenyl **18** to the *carbo*-stilbene **8a** suggesting the largest  $\pi$ -conjugation extent including the two phenyl substituents of the DAB bridge as compared to **8b**.

By comparison to *carbo*-biphenyl **18** (Figure 3), the UV-vis absorption spectrum of **8b** is slightly broader but not markedly resolved for the *cis* and *trans* isomers, tending to preclude significant photochromic behavior (see discussion in ref<sup>[1c]</sup> and references therein). For **8a**, while the second and third absorption bands of the *cis* and *trans* forms remain unresolved (at 553 and 735 nm), the maximum band at 455 nm is accompanied by a shoulder red-shifted by  $\Delta\lambda = +20$  nm at 475 nm. This shoulder could actually be attributed to *cis*-**8a** by reference to the TD-DFT calculated values  $\lambda_{\text{calcd}}(\text{trans-8a}) = 470$  nm and  $\lambda_{\text{calcd}}(\text{cis-8a}) = 484$  nm, with  $\Delta\lambda_{\text{calcd}} = 14$  nm (Table S1). Indeed, at the CAM-B3LYP-D3/6-311G(d,p)-smd(chloroform)//B3PW91/6-31G(d,p) time dependent DFT level, calculated absorption spectra reproduced the experimental ones in Figure 3, in particular the bathochromic displacement of the highest wavelength band for **8a** and **8b** with respect to **18** (see Table S1). This band is actually mainly associated to the HOMO→LUMO transition. The corresponding gap decreases from 3.42 eV for **18** to 3.34 and 3.20 eV for **8b** and **8a**, respectively, averaging the *cis*- and *trans*-conformations to take into account the coexistence of both. Going into detail, with respect to **18**, the HOMO of **8a** and **8b** destabilizes by 0.13 and 0.11 eV, respectively. The LUMO shows a disparate behavior: for **8b** it also destabilizes, by 0.03 eV, while for **8a** it stabilizes by 0.09 eV (see Table S2). This last factor accounts for the accentuated bathochromic shift of **8a** vs **8b**.

The electrochemical behavior of the *carbo*-stilbenes **8b** and **8a** was also studied by square wave voltammetry (Figure 4 and S.I.). Their low solubility did not allow satisfactory results in cyclic voltammetry. For still poor solubility reasons, the measurements were performed after deposition on the working electrode by dipping in a chloroform solution of **8b** or **8a**. Because of this unconventional method, only the first oxidation and reduction potentials could be determined (Table 1 and S.I.). In these conditions, a *quasi*-reversible reduction was observed at  $E_{1/2} = -0.63$  V/SCE (**8b**) or  $E_{1/2} = -0.53$  V/SCE (**8a**), and an irreversible oxidation was evidenced at 1.06 V/SCE (**8b**) or  $E_{1/2} = 1.04$  V/SCE (**8a**). These results are in agreement with those previously obtained for other tetraphenyl-*carbo*-benzene derivatives, and in particular the *carbo*-biphenyl **18**, exhibiting a first reduction potential at  $-0.58$  V/SCE.<sup>[21]</sup> The low reduction

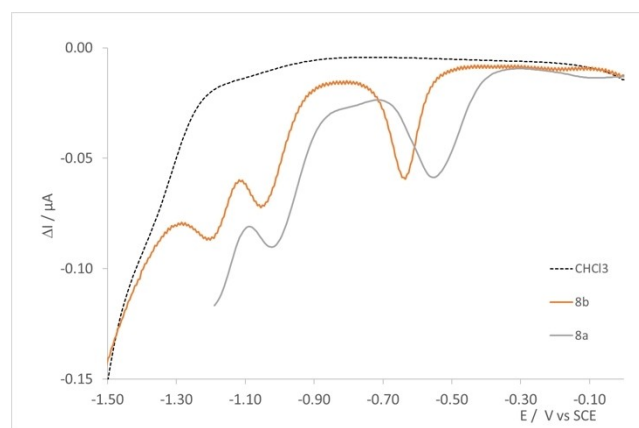


**Figure 4.** Square-wave voltammograms (reduction scan) of **8a** and **8b** deposited on Pt electrode in electrolytic solution:  $\text{CHCl}_3$  (10 mL) + 0.1 M  $[\text{tBu}_4\text{N}][\text{PF}_6]$  at  $0.1 \text{ V}\cdot\text{s}^{-1}$ . Oxidation scan in the S.I.

**Table 1.** Electrochemical data for **8a** and **8b** deposited on a Pt microdisk at room temperature in  $\text{CHCl}_3$ , 0.1 M  $[\text{tBu}_4\text{N}][\text{PF}_6]$  as supporting electrolyte. Potential values in V/SCE.

	$E_{1/2}$ red 3	$E_{1/2}$ red2	$E_{1/2}$ red1	$E_{1/2}$ ox1	$E_{1/2}$ ox2
<b>8b</b>	-1.19	-1.04	-0.63	1.06	(1.22)**
<b>8a</b>	(-1.19)**	-0.99	-0.53	1.04*	1.28*

\* shoulder. \*\* Uncertain values (see Figures 4 and S4.2).

potentials of both **8b** and **18** are consistent with their extended  $\pi$ -conjugated systems.

## Conclusions

In spite of many attempts, the failure to obtain single crystals of the *carbo*-stilbenes **8a** and **8b** with a suitable quality for X-ray diffraction analysis can be attributed to the presence of *quasi*-equal amounts of the *cis*- and *trans*-isomers, which could not be separated by either fractional crystallization or preparative chromatography. The absence of crystallographic characterization was however superseded by DFT calculations at suitable level allowing mimicry of experimental conditions, in particular by using the B3PW91-D3 and CAM-B3PYP-D3 functionals taking into account dispersive effects, and the PCM method taking into account a dichloromethane solvent medium.

The disclosed results extend the knowledge on oligo-*carbo*-benzenic derivatives, illustrating further the basic relevance of *carbo*-mer chemistry, and paving the way to future developments.

For example, in spite of the fact that the exemplified *cis*- and *trans*-*carbo*-stilbenes are *quasi*-isoenergetic, a next challenge would be to achieve some stereochemical control, e.g. by photo-isomerization at proper wavelengths, as in the case of parent stilbenes.<sup>[1,3]</sup>

Although the Oki temperature<sup>[29]</sup> of the first *carbo*-stilbenes **8a–b** remains unknown, it should be possible to trigger the *cis*

⇌ *trans* interconversion photochemically, or even thermally above 80 °C. Under such conditions, or by a natural kinetic control during the last step of the synthesis (**17 a–b** + 7 SnCl<sub>2</sub> → **8 a–b** + 7 SnCl<sub>2</sub>X<sub>2</sub>, X = OH, OMe, see Scheme 2), a way to favor the *trans*-isomer would be to implement “bulky phenyl substituents” at the *carbo*-benzene rings (e.g. mesityl groups), as recently illustrated for a related geometrical control of helical polyanthracenes.<sup>[30]</sup> Alternatively, the *cis*-isomers might be favored by hydrogen bonding between hydroxylated phenyl substituents.

An ultimate way to favor *cis*-isomers would require the challenging synthesis of dissymmetric *carbo*-stilbenes with the view to enhancing  $\pi$ -stacking of complementary aryl substituents by charge transfer, e.g. between C<sub>6</sub>H<sub>4</sub>NO<sub>2</sub> and C<sub>6</sub>H<sub>4</sub>NMe<sub>2</sub> groups. Even in the *trans* geometry, such donor-acceptor *carbo*-stilbenes could exhibit significant values of quadratic hyperpolarizability for applications in nonlinear optics, such as second harmonic generation, just as earlier predicted for donor-acceptor-substituted *carbo*-benzenes.<sup>[31]</sup>

## Acknowledgements

A.P. is a Serra Hünter Fellow and ICREA Academia Prize 2019, and thanks the Spanish Ministerio de Ciencia e Innovación for project PID2021-127423NB-I00 and the Generalitat de Catalunya for project 2021SGR623. C.Z. thanks the China Scholarship Council for his Ph.D. scholarship. V.M. thanks The Centre National de la Recherche Scientifique (CNRS). The work was partly performed thanks to funding from the Agence Nationale de la Recherche, which is acknowledged for supporting the related projects ANR-11-BS07-016-01 and ANR-18-CE06-00029-01.

## Conflict of Interests

The authors declare no conflict of interest.

## Data Availability Statement

The data that support the findings of this study are available in the supplementary material of this article.

**Keywords:** aromaticity · *carbo*-benzene · DFT calculations · *carbo*-stilbene · stilbene

- [1] Fore recent reviews on stilbene derivatives, see: a) *Stilbenes: Applications in Chemistry, Life Sciences and Materials Science*, G. Likhtenshtein, Wiley-VCH, Weinheim, 2009; b) E. A. Abourashed, *J. Nat. Prod.* **2017**, *80*, 577; c) D. Villaron, S. J. Wezenberg, *Angew. Chem. Int. Ed.* **2020**, *59*, 13192–13202; d) F. Doraghi, F. Yousefnejad, S. Farzipour, S. P. Aledavoud, B. Larjani, M. Mahdavi, *Org. Biomol. Chem.* **2023**, *21*, 1846–1861, and references therein.
- [2] See for example: a) ref [1a] pp. 189–223; b) Y. Wang, Y. Jiang, X. Fan, H. Tan, H. Zeng, Y. Wang, P. Chen, M. Huang, H. Bi, *Toxicol. Lett.* **2015**, *236*, 82–89; c) E. Giacomini, S. Rupiani, L. Guidotti, M. Recanatini, M. Roberti,

- Curr. Med. Chem.* **2016**, *23*, 2439–2489; d) H. M. Wahedi, S. Ahmad, S. W. Abbasi, *J. Biomol. Struct. Dyn.* **2021**, *39*, 3225–3234; e) J.-Y. Chen, X. Lian, Y.-W. Fan, Z.-Y. Ao, W. J. Zhang, Y.-C. Pan, L.-P. Chen, J. Yuan, J.-W. Wu, *J. Nat. Med.* **2023**, *77*, 858–866; f) C.-G. Duta-Bratu, G. M. Nitulescu, D. P. Mihai, O. T. Olaru, *Plants* **2023**, *12*, 2935; g) M. Kluska, J. Jablonska, W. Prukala, *Molecules* **2023**, *28*, 4482, and references therein.
- [3] See for example: a) ref [1a] pp. 159–188; b) M. Cao, X. Chen, K. Yi, D. Wei, *J. Phys. Chem. C* **2017**, *5*, 9597–9601; c) E. Kukkonen, E. Lahtinen, P. Myllyperkio, M. Haukka, J. Konu, *New J. Chem.* **2021**, *45*, 6640–6650; d) D. Zhang, H. Zhu, X. Sheng, *Phys. Chem. Chem. Phys.* **2023**, *25*, 7508–7518; e) Y.-G. Lee, J.-H. Choi, *Appl. Sci.* **2023**, *13*, 5543 (1–14); f) J. Rouillon, C. Andraud, C. Monnereau, *ChemRxiv.* **2023**, doi:10.26434/chemrxiv-2023-b9x37, and references therein.
- [4] a) The term “*carbo*(–)m(M)er” has actually 3 different namesakes and spellings: (i) as understood in this article, an etymology-based name for a category of chemical structures defined in 1995,<sup>[4b]</sup> which was hyphenated in 2003,<sup>[4h]</sup> before being spelled, in 2004,<sup>[4i]</sup> with an italicized “*carbo*–” descriptor similar to standard Greek prefixes (*mono*-, *oligo*-, *poly*-, *iso*-...), non-figure locants (*ortho*-, *meta*-, *para*-,  $\alpha$ -,  $\beta$ -,  $\gamma$ -,  $\omega$ -...) or stereochemical indicators (*cis*-, *trans*-, *syn*-, *anti*-, *meso*-, *threo*-, *erythro*-...); (ii) a commercial trademark with the one-piece spelling “*carbomer*”, coined for hydrophilic polyacrylic gels used as emulsifying or thickening agents in cosmetics or toiletry products; (iii) an industrial company name with the doubly capitalized spelling “*CarboMer*”, leader in carbohydrate and polymer technology with extensive expertise in materials sciences (https://carbomer.com/); for early papers and reviews, see: b) Y. Kuwatani, N. Watanabe, I. Ueda, *Tetrahedron Lett.* **1995**, *36*, 119–122; c) R. Chauvin, *Tetrahedron Lett.* **1995**, *36*, 397–400; d) R. Suzuki, H. Tsukuda, N. Watanabe, Y. Kuwatani, I. Ueda, *Tetrahedron* **1998**, *54*, 2477–2496; e) V. Maraval, R. Chauvin, *Chem. Rev.* **2006**, *106*, 5317–5343; f) K. Cocq, C. Lepetit, V. Maraval, R. Chauvin, *Chem. Soc. Rev.* **2015**, *44*, 6535–6559; g) K. Cocq, C. Barthes, A. Rives, V. Maraval, R. Chauvin, *Synlett* **2019**, *30*, 30–43; h) C. Lepetit, M. B. Nielsen, F. Diederich, R. Chauvin, *Chem. Eur. J.* **2003**, *9*, 5056–5066; i) C. Lepetit, V. Peyrou, R. Chauvin, *Phys. Chem. Chem. Phys.* **2004**, *6*, 303–309.
- [5] a) Cocq, N. Saffon-Merceron, Y. Coppel, C. Poidevin, V. Maraval, R. Chauvin, *Angew. Chem. Int. Ed.* **2016**, *55*, 15133–15136; b) J. Poater, J. Heitkampfer, A. Poater, V. Maraval, R. Chauvin, *Eur. J. Org. Chem.* **2021**, 6450–6458.
- [6] C. Zhu, A. Poater, C. Duhayon, B. Kauffmann, A. Saquet, V. Maraval, R. Chauvin, *Angew. Chem. Int. Ed.* **2018**, *57*, 5640–5644.
- [7] E. L. Eliel, S. H. Wilen, M. P. Doyle, *Basic Organic Stereochemistry*, 16th Ed, Wiley, 2001.
- [8] a) J. A. Januszewski, D. Wendinger, C. D. Methfessel, F. Hampel, R. R. Tykwinski, *Angew. Chem. Int. Ed.* **2013**, *52*, 1817–1821; b) D. Wendinger, R. R. Tykwinski, *Acc. Chem. Res.* **2017**, *50*, 1468–1479.
- [9] J. E. Barquera-Lozada, *Chem. Eur. J.* **2020**, *26*, 4633–4639.
- [10] a) Assuming a singlet spin state, the Pauli exclusion principle repels the unpaired electrons to the ends of the chain; b) The CRB of a [2m]cumulene is much higher than that of the shorter [2m–1]cumulene due to the 4-electron octet-deficient carbenic form R<sup>1</sup>R<sup>2</sup>C<sup>•</sup>–(C≡C)<sub>m–1</sub>–C–C<sup>•</sup>R<sup>1</sup>R<sup>2</sup> vs the 2-electron octet-deficient form R<sup>1</sup>R<sup>2</sup>C<sup>•</sup>–(C≡C)<sub>m–1</sub>–C<sup>•</sup>R<sup>1</sup>R<sup>2</sup>.
- [11] L. Leroyer, V. Maraval, R. Chauvin, *Chem. Rev.* **2012**, *112*, 1310–1343.
- [12] P. D. Jarowski, F. Diederich, K. N. Houk, *J. Phys. Chem. A* **2006**, *110*, 7237–7246.
- [13] P. Gawel, Y.-L. Wu, A. D. Finke, N. Trapp, M. Zalibera, C. Boudon, J.-P. Gisselbrecht, W. B. Schweizer, G. Gescheidt, F. Diederich, *Chem. Eur. J.* **2015**, *21*, 6215–6225.
- [14] A. Auffrant, B. Jaun, P. D. Jarowski, K. N. Houk, F. Diederich, *Chem. Eur. J.* **2004**, *10*, 2906–2911.
- [15] J.-D. van Loon, P. Seiler, F. Diederich, *Angew. Chem. Int. Ed.* **1993**, *32*, 1187–1189.
- [16] A. Auffrant, F. Diederich, C. Boudon, J.-P. Gisselbrecht, M. Gross, *Helv. Chim. Acta* **2004**, *87*, 3085–3105.
- [17] V. Maraval, L. Leroyer, A. Harano, C. Barthes, A. Saquet, C. Duhayon, T. Shinmyozu, R. Chauvin, *Chem. Eur. J.* **2011**, *17*, 5086–5100.
- [18] A. Rives, V. Maraval, N. Saffon-Merceron, R. Chauvin, *Chem. Eur. J.* **2012**, *18*, 14702–14707.
- [19] A. Rives, V. Maraval, N. Saffon-Merceron, R. Chauvin, *Chem. Eur. J.* **2014**, *20*, 483–492.
- [20] A. Rives, I. Baglai, C. Barthes, V. Maraval, N. Saffon-Merceron, A. Saquet, Z. Voitenko, Y. Volovenko, R. Chauvin, *Chem. Sci.* **2015**, *6*, 1139–1149.
- [21] C. Barthes, A. Rives, V. Maraval, E. Chelain, T. Brigaud, R. Chauvin, *Fr. Ukr. J. Chem.* **2015**, *3*, 60–65.

- [22] C. Zhu, A. Poater, C. Duhayon, B. Kauffmann, A. Saquet, V. Maraval, A. Rives, R. Chauvin, *Chem. Eur. J.* **2021**, *27*, 9286–9291.
- [23] R. Chauvin, *Tetrahedron Lett.* **1995**, *36*, 401–404.
- [24] L. Leroyer, C. Zou, V. Maraval, R. Chauvin, *C. R. Chim.* **2009**, *12*, 412–429.
- [25] D. Listunov, C. Duhayon, A. Poater, S. Mazerès, A. Saquet, V. Maraval, R. Chauvin, *Chem. Eur. J.* **2018**, *24*, 10699–10710.
- [26] a) P. v. R. Schleyer, C. Maerker, A. Dransfeld, H. Jiao, N. J. R. van Eikema Hommes, *J. Am. Chem. Soc.* **1996**, *118*, 6317–6318; b) Z. Chen, C. S. Wannere, C. Corminboeuf, R. Puchta, P. v. R. Schleyer, *Chem. Rev.* **2005**, *105*, 3842–3888.
- [27] Examples of NICS applications in different nature and ring sizes, where NICS values are not normalized: a) P. D. Listunov, O. Hammerich, I. Caballero-Quintana, A. Poater, C. Barthes, C. Duhayon, M. H. Larsen, J.-L. Maldonado, G. Ramos-Ortiz, M. B. Nielsen, V. Maraval, R. Chauvin, *Chem. Eur. J.* **2020**, *26*, 10707–10711; b) A. Poater, S. Moradell, E. Pinilla, J. Poater, M. Solà, M. A. Martínez, A. Llobet, *Dalton Trans.* **2006**, 1188–1196; c) A. Poater, X. Ribas, A. Llobet, L. Cavallo, M. Solà, *J. Am. Chem. Soc.* **2008**, *130*, 17710–17717; d) R. Credendino, A. Poater, F. Ragone, L. Cavallo, *Catal. Sci. Technol.* **2011**, *1*, 1287–1297; e) J. Poater, M. Gimferrer, A. Poater, *Inorg. Chem.* **2018**, *57*, 6981–6990; f) J. Poater, S. Escayola, A. Poater, F. Teixidor, H. Ottosson, C. Viñas, M. Solà, *J. Am. Chem. Soc.* **2023**, *145*, 22527–22538.
- [28] F. Feixas, E. Matito, J. Poater, M. Solà, *J. Comput. Chem.* **2008**, *29*, 1543–1554.
- [29] M. Oki in *Topics in Stereochemistry*, Vol. 14 (Eds.: N. L. Allinger, E. L. Eliel, S. H. Wilen), Wiley, New York, 1983, pp. 1–81.
- [30] K. Suzuki, H. Fukuda, H. Toda, Y. Imai, Y. Nojima, M. Hasegawa, E. Tsurumaki, S. Toyota, *Tetrahedron* **2023**, *132*, 133243.
- [31] a) J.-M. Ducere, C. Lepetit, P. G. Lacroix, J.-L. Heully, R. Chauvin, *Chem. Mater.* **2002**, *14*, 3332–3338; b) C. Lepetit, P. G. Lacroix, V. Peyrou, C. Saccavini, R. Chauvin, *J. Comput. Methods Sci. Eng.* **2004**, *4*, 569–588.

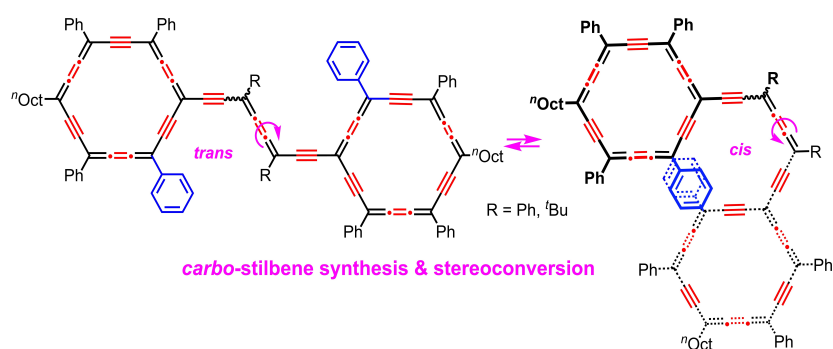
---

Manuscript received: January 31, 2024

Accepted manuscript online: February 26, 2024

Version of record online: ■■, ■■





Dr. C. Zhu, Dr. A. Saquet, Dr. V. Maraval, Dr. C. Bijani, Prof. X. Cui, Dr. A. Poater\*, Prof. R. Chauvin\*

1 – 8

From Stilbenes to *carbo*-Stilbenes: an Encouraging Prospect



Two novel bis-*carbo*-benzenic molecules, derived from the stilbene parent, are explored beyond *carbo*-naphthalene and *carbo*-biphenyl. The synthesis, structure, and properties of these *carbo*-stilbenes are investigated using experimental and computational methods. The molecules exhibit iso-

merization, with *cis*- and *trans*-isomers, and the calculated *cis*-isomer shows a helical structure. The UV-vis spectra display broad bands, and voltammograms indicate classical behavior for *carbo*-benzene derivatives.